

# Beam and Experiments: Summary

A. Blondel, A. Bueno, M. Campanelli, A. Cervera, D.B. Cline,  
J. Collot, M. de Jong, A. Donini, F. Dydak, R. Edgecock,  
M.B. Gavela, J.J. Gómez-Cadenas, M.C. Gonzalez-Garcia,  
P. Gruber, D.A. Harris, P. Hernández, Y. Kuno, P.J. Litchfield,  
K. McFarland, O. Mena, P. Migliozzi, V. Palladino, J. Panman,  
I.M. Papadopoulos, A. Para, C. Peña-Garay, P. Perez,  
S. Rigolin, A. Romanino, A. Rubbia, P. Strolin, S. Wojcicki

---

## Abstract

The discovery of neutrino oscillations marks a major milestone in the history of neutrino physics, and opens a new window to the still mysterious origin of masses and flavour-mixing. Many current and forthcoming experiments will answer open questions; however, a major step forward, up to and possibly including CP violation in the neutrino-mixing matrix, requires the neutrino beams from a neutrino factory. The neutrino factory is a new concept for producing neutrino beams of unprecedented quality in terms of intensity, flavour composition, and precision of the beam parameters. Most importantly, the neutrino factory is the only known way to generate a high-intensity beam of electron neutrinos of high energy. The neutrino beam from a neutrino factory, in particular the electron-neutrino beam, enables the exploration of otherwise inaccessible domains in neutrino oscillation physics by exploiting baselines of planetary dimensions. Suitable detectors pose formidable challenges but seem within reach with only moderate extrapolations from existing technologies. Although the main physics attraction of the neutrino factory is in the area of neutrino oscillations, an interesting spectrum of further opportunities ranging from high-precision, high-rate neutrino scattering to physics with high-intensity stopped muons comes with it.

*Key words:* NUFACT99 ; neutrino ; oscillations ; Lyon ; Beaujolais

---

## 1 Introduction

The neutrino factory is, in essence, a muon storage ring with long straight sections along which decaying muons produce well-defined neutrino beams. The idea is a natural offspring of the concept of a muon collider, first proposed by Budker (1) at the 1969 Yerevan Conference, and developed further by

Skrinsky (2). The first proposal for a genuine neutrino factory was put forward in quite some detail as early as 1974 by Koshkarev (3). The concept of a neutrino factory was also discussed around that time at Fermilab by Wojcicki and Collins (4).

It was not until the 1990s that the idea of the muon collider was again taken up, this time going well beyond the level of studies on paper. The US-led Muon Collider Collaboration (5) developed a conceptual layout of a multi-TeV muon collider, including all stages from muon production to the storage of high-energy muons in a circular collider, and launched an ambitious R&D programme.

In the context of this work, the old idea of a neutrino factory was developed further and highlighted in a comprehensive paper by Geer (6). A workshop was held at Fermilab in 1997 which addressed in quite some detail already the physics which was possible at the front end of a muon collider (7). Shortly thereafter, in 1998, the concept of the neutrino factory was also vigorously taken up by a study group in Europe (8). This group's work became rapidly an ECFA-sponsored activity.

The study of the physics and machine aspects of the neutrino factory began to take a worldwide dimension. Interested groups in Europe, Japan and the USA started to collaborate and to harmonize their R&D programmes. This workshop marks a first culmination of these efforts.

The neutrino fluxes from the neutrino factory are much higher than achieved before and have a well-defined flavour composition, free of background. These characteristics made physicists think about neutrino oscillation measurements in a new way. Distances between production and detection can now span the planet, and given the flavour composition of the beam, one can map out a plan to measure the neutrino-mixing matrix much like physicists now are measuring the CKM quark-mixing matrix. Alternatively, one can also think about putting experiments extremely close to the production location, and using these extremely intense neutrino beams to map out nuclear structure much like electron and muon beams have done in the past.

This report from the workshop's 'Beam and Experiments' session, but in part also from work done by working groups continuing after the workshop, summarizes the oscillation physics questions which can be addressed at the neutrino factory and discusses the choice of beam parameters as well as detector issues that would be most relevant for neutrino oscillation measurements. As an example of how diverse a neutrino programme at the neutrino factory could be, highlights of possible nucleon structure and other 'near' detector measurements are also given.

## 2 Neutrino beams: the new versus the old concept

The neutrino beams of the neutrino factory originate from the decay of high-momentum muons along straight sections of a storage ring:

$$\mu^+ \rightarrow e^+ \nu_e \bar{\nu}_\mu \quad \text{and} \quad \mu^- \rightarrow e^- \bar{\nu}_e \nu_\mu$$

In Table 1 a comparison is made between a conventional magnetic horn-focused muon neutrino beam from pion and kaon decay, and a beam from the neutrino factory (in the latter case on the assumption that diluting effects from the angular divergence and the polarization of the muon beam are well under control). The comparison is made specifically for the NGS beam (9) from CERN to the Laboratorio Nazionale del Gran Sasso 732 km away (the twin companion of the beam from Fermilab to the Soudan mine in Minnesota), with a neutrino factory sending a beam over the same distance. The situation is discussed in more detail by Palladino (10).

Table 1

Comparison of a conventional neutrino beam with the beam from a neutrino factory.

	Conventional	Neutrino factory
Parents	$\pi^+, K^+$ or $\pi^-, K^-$	$\mu^-$ or $\mu^+$
$\nu_\mu$ beam	$\nu_\mu$	$\nu_\mu : \bar{\nu}_e = 1 : 1$
Background	$\sim 2\%$ of $\bar{\nu}_\mu$ , $\sim 1\%$ of $\nu_e$	none
$\bar{\nu}_\mu$ beam	$\bar{\nu}_\mu$	$\bar{\nu}_\mu : \nu_e = 1 : 1$
Background	$\sim 6\%$ of $\nu_\mu$ , $\sim 0.5\%$ of $\bar{\nu}_e$	none
$\Delta E/E$ of neutrino energy	$\pm 10\%$	$< 1\%$
$\Delta R/R$ of neutrino radius	$\pm 10\%$	$< 1\%$
neutrino flux uncertainty	$\pm 10\%$	$< 1\%$
$\nu_\mu$ per $\text{cm}^2$ per year at 732 km	$3 \times 10^7$ for $4.5 \times 10^{19}$ 400 GeV/c p.o.t.	$3 \times 10^9$ for $10^{21}$ injected 50 GeV/c $\mu$

The decisive difference between the neutrino beam from the neutrino factory and the conventional beam is not so much the high beam intensity, since with a proton driver of comparable power a conventional neutrino beam would have a comparably high  $\nu_\mu$  intensity. The difference is rather the well-defined and intense  $\nu_e$ -beam which is not available by other means and which opens the

window to important physics questions which, as will be discussed below, are considered not accessible with a  $\nu_\mu$  beam.

### 3 Neutrino factory: machine aspects for pedestrians

The current ideas about the accelerator network associated with the neutrino factory have been shaped considerably at this workshop. Whereas before the workshop three different designs existed, a unified design has now been agreed upon, the only remaining difference being the proton driver. Even there the beam power on target (which is the relevant quantity for the production of charged pions) has been agreed upon: 4 MW, for experts quite a daring but not unrealistic figure. This figure is important as it limits the number of injected muons to  $\sim 10^{21}$  per year, which, since this workshop, is considered the baseline figure. However, it is recognized that the physics (in particular CP violation) in all likelihood will ask for more, so  $10^{22}$  injected muons per year is retained as an option to be kept in mind.

A very schematic layout of the neutrino factory complex is shown in Fig. 1 with a view to illustrating its salient features. As for details, the reader is referred to the many contributions on this subject to this workshop, and in particular to the overall design proposed by Palmer et al. (11).

The protons deliver a power of 4 MW onto a high- $Z$  target. The target technology is very difficult, as very strong pressure waves have to be sustained. Also, a high amount of heat must be transported away from the target, as  $\sim 25\%$  of the beam power is dissipated in the target. The target is embedded in a strong solenoidal field of some 20 T. The accepted forward-going pions are phase-rotated, i.e. their momentum spread is reduced at the cost of bunch lengthening. After a drift space where the pions decay, the decay muons are ‘cooled’ with a relatively moderate compression of the six-dimensional phase space by a factor of 75. Since muons are unstable (lifetime  $\tau_\mu = 2.2 \mu\text{s}$ ), all further actions on them must be highly efficient so as to accelerate them as quickly as possible to their final momentum, thus profiting to a maximum from Lorentz time dilation ( $\beta\gamma\tau_\mu = 1.0 \text{ ms}$  for circulating muons of 50 GeV/ $c$  momentum).

The cooled muons are first accelerated to  $\sim 2 \text{ GeV}$ , then they enter two recirculating linacs, where they are repeatedly accelerated in a straight section, and returned in recirculating arcs. Each arc is optimized for a certain momentum, rendering a number of discrete arcs necessary. For physics reasons, a momentum range up to 50 GeV/ $c$  is desired, where 50 GeV/ $c$  is a limit imposed by financial considerations rather than by physics objectives.

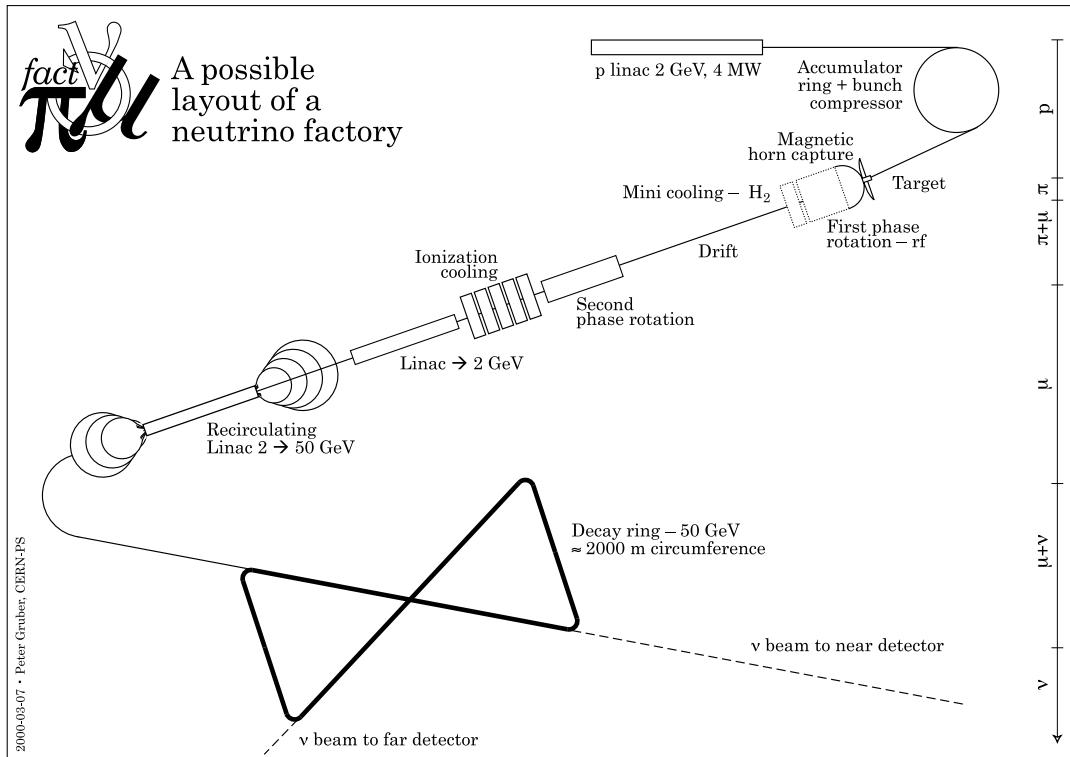


Fig. 1. Generic layout of the neutrino factory complex.

Finally, the muons enter the muon storage ring. It has two straight sections, each pointing to ‘far’ detectors at different distances (say 732 and 5000 km), implying inclination angles of  $3^\circ$  and  $23^\circ$ , respectively. The arcs are as short as possible. The two straight sections and the arcs are arranged in a near-planar geometry. One or several ‘near’ detectors would be located at the end of one straight section.

While the overall design is considered feasible by the experts, it is recognized that a lot of R&D work must be successfully accomplished before a serious engineering design can be made. Particularly critical areas are the target zone and the muon cooling. Accordingly, the next few years are expected to be busy with a variety of dedicated R&D experiments.

#### 4 Neutrinos from beams of unpolarized and polarized muons

The decay of the muon is a well-known and precisely calculable process. In the muon rest frame, the distribution of muon antineutrinos (neutrinos) and electron neutrinos (antineutrinos) in the decay  $\mu^\pm \rightarrow e^\pm + \nu_e(\bar{\nu}_e) + \bar{\nu}_\mu(\nu_\mu)$  is

given by:

$$\frac{d^2 N}{dx d\Omega} = \frac{1}{4\pi} [f_0(x) \mp P_\mu f_1(x) \cos \theta],$$

where  $E_\nu$  denotes the neutrino energy,  $x = 2E_\nu/m_\mu$ , and  $P_\mu$  is the average muon polarization along the muon beam direction (12).  $\theta$  is the angle between the neutrino momentum vector and the muon spin direction and  $m_\mu$  is the muon mass. The positron (electron) spectrum is identical to that for muon neutrinos (antineutrinos), when the electron mass is neglected. The functions  $f_0$  and  $f_1$  are given in Table 2.

Table 2

Flux functions in the muon rest-frame.

	$f_0(x)$	$f_1(x)$
$\nu_\mu, e$	$2x^2(3 - 2x)$	$2x^2(1 - 2x)$
$\nu_e$	$12x^2(1 - x)$	$12x^2(1 - x)$

The neutrino energy spectrum in  $\mu^+$  decay is shown in Fig. 2 for unpolarized muons, together with the monoenergetic line of  $\nu_\mu$  in  $\pi^+$  decay. While the  $\bar{\nu}_\mu$  spectrum (which is the same as the positron spectrum) peaks at the kinematic limit of 53 MeV, the  $\nu_e$  spectrum is a bit softer and peaks at 2/3 of it. The neutrinos from muons decaying in the straight sections are Lorentz-boosted in the forward direction towards the detector which is located at some distance  $L$ . The neutrino flux in the forward direction is proportional to  $E_\mu^2/L^2$ , and half of the neutrinos are contained within a cone angle of  $1/(\beta\gamma) = m_\mu/p_\mu$ . As the detector will be located at a distance of hundred kilometres or even more, it will be very much smaller than the transverse size of the beam. Taking into account the neutrino cross-section which rises linearly with energy, the event rate in the detector scales with  $M \times E_\mu^3/L^2$ , where  $M$  is the fiducial target mass of the detector.

The energy spectrum of the neutrino flux in the distant detector is the same as shown in Fig. 2, but with the energy scale multiplied by the Lorentz boost factor  $2E_\mu/m_\mu$ .

Because of the well-defined helicities of the decay particles in muon decay, there is a strong correlation between the direction of emission and the muon-polarization vector. The  $\nu_e$  ( $\bar{\nu}_e$ ) plays a special rôle insofar as its helicity is opposite to that of the other two particles, the positron (electron) and  $\bar{\nu}_\mu$  ( $\nu_\mu$ ). This means, in the decay  $\mu^+ \rightarrow e^+ \nu_e \bar{\nu}_\mu$  for example, that the  $\nu_e$ 's are always emitted in the opposite direction to the muon-polarization vector, so that they can never reach the 'far' detector other than with negligible

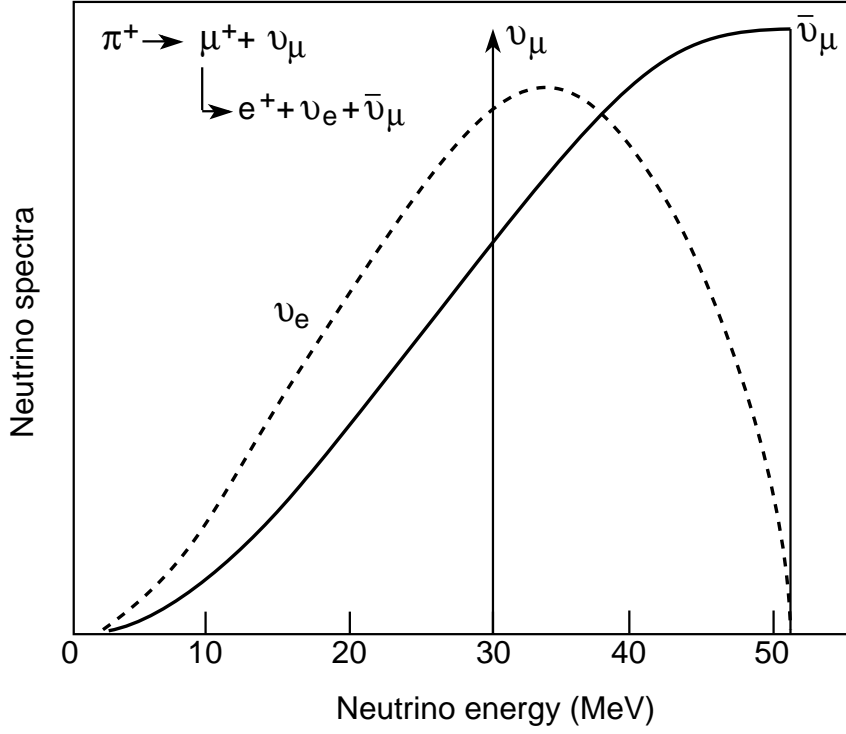


Fig. 2. Neutrino energy spectra from  $\pi^+$  and  $\mu^+$  decay in the rest frames.

energy. Table 3 summarizes the situation for both muon polarities and both polarization states: unlike  $\nu_\mu$ ,  $\nu_e$  can be ‘switched off’ by a 100% polarization of the right sign.

Table 3

Neutrino beam composition for different muon polarization.

	$P = +1$	$P = -1$
$\mu^+$	only $\bar{\nu}_\mu$	$\nu_e + \bar{\nu}_\mu$
$\mu^-$	$\bar{\nu}_e + \nu_\mu$	only $\nu_\mu$

Fig. 3 taken from Ref. (13) shows the event spectra in a detector located 732 km away from the neutrino factory, for  $\mu^+ \rightarrow e^+ \nu_e \bar{\nu}_\mu$  beams of 50 GeV/c. The sensitivity of the spectra to the muon polarization is striking.

Also, since the  $\nu_e$  ( $\bar{\nu}_e$ ) is always emitted together with a second particle in the same direction, it never attains the maximum energy permitted by the kinematic limit. This opens the way in principle to look near the kinematic

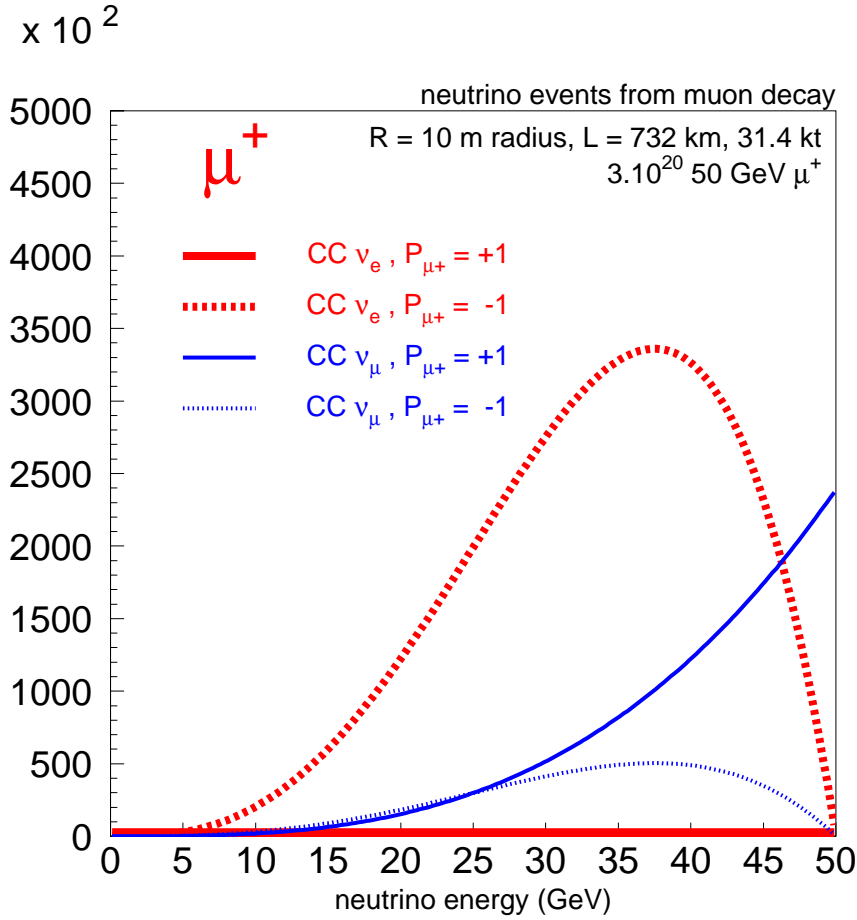


Fig. 3. Event spectra for different muon beam polarizations in a detector located 732 km away from the neutrino factory for  $\mu^+ \rightarrow e^+ \nu_e \bar{\nu}_\mu$  beams of 50 GeV/c. The energy spread and the divergence of the muon beam are both assumed as zero.

limit for the appearance of  $\nu_e$  ( $\bar{\nu}_e$ ), which could then only be the result of an oscillation of  $\nu_\mu$  ( $\bar{\nu}_\mu$ ) into  $\nu_e$  ( $\bar{\nu}_e$ ). While this strategy is already possible with unpolarized muons, it improves considerably with muon-polarization. Therefore, having a large degree of polarization is potentially of great interest (14), as it could circumvent our current inability to build multi-kiloton detectors able to distinguish the interactions of  $\nu_e$  and  $\bar{\nu}_e$ , relevant for the search for CP violation in the neutrino-mixing matrix.

## 5 Neutrino oscillation physics challenges

The physics case for the neutrino factory is largely – but not solely – driven by neutrino oscillations.

### 5.1 What do we know and what are the open questions?

The atmospheric (15; 16) and solar (17) neutrino data point strongly to neutrino oscillations (18; 19) and can be easily accommodated in a pessimistic yet largely accepted three-family mixing scenario.

Let  $U$ , with  $(\nu_e, \nu_\mu, \nu_\tau)^T = U \cdot (\nu_1, \nu_2, \nu_3)^T$ , be the neutrino-mixing matrix in the conventional parametrization (20):

$$U \equiv \begin{pmatrix} 1 & 0 & 0 \\ 0 & c_{23} & s_{23} \\ 0 & -s_{23} & c_{23} \end{pmatrix} \begin{pmatrix} c_{13} & 0 & s_{13}e^{i\delta} \\ 0 & 1 & 0 \\ -s_{13}e^{-i\delta} & 0 & c_{13} \end{pmatrix} \begin{pmatrix} c_{12} & s_{12} & 0 \\ -s_{12} & c_{12} & 0 \\ 0 & 0 & 1 \end{pmatrix}$$

with  $s_{12} \equiv \sin \theta_{12}$ , and similarly for the other sines and cosines. The action of the three rotation matrices is illustrated in Fig. 4.

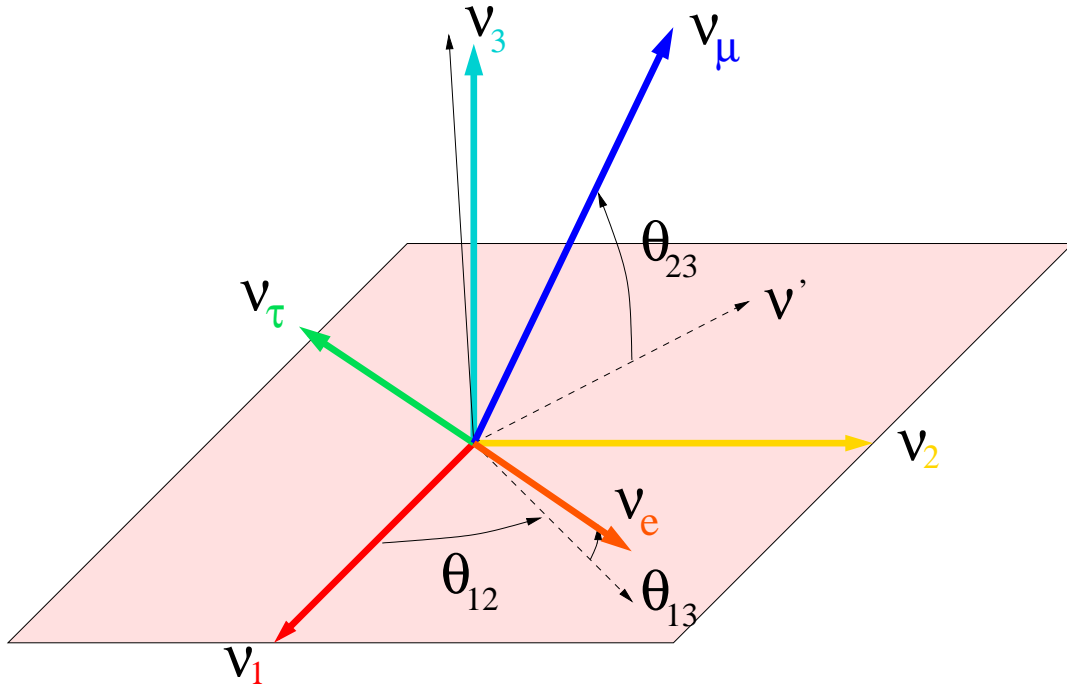


Fig. 4. Rotation between the mass and flavour eigenstates in the three-family neutrino oscillation scheme.

Oscillation experiments are sensitive to six independent parameters: two mass-squared differences  $\Delta m_{12}^2$  and  $\Delta m_{23}^2$ , and the four parameters in the above mixing matrix, three angles  $\theta_{12}$ ,  $\theta_{13}$ ,  $\theta_{23}$ , and the CP-violating phase  $\delta$ .

Our perceived state of knowledge is:

- The solar neutrino deficit is interpreted either as MSW (matter enhanced) oscillations (19) or as vacuum oscillations (VO) (18) that deplete the original  $\nu_e$ 's, presumably in favour of  $\nu_\mu$ 's or alternatively into sterile neutrinos. The corresponding squared mass differences –  $O(10^{-5}\text{--}10^{-4})$  eV<sup>2</sup> for the large mixing angle MSW solution (LMA-MSW),  $O(10^{-6})$  eV<sup>2</sup> for the small mixing angle MSW solution (SMA-MSW), or  $O(10^{-10})$  eV<sup>2</sup> for VO – are significantly below the range deduced from atmospheric-neutrino observations. This mass difference is identified with  $\Delta m_{12}^2$ .
- The SuperKamiokande data on atmospheric neutrinos, presented by Hayato (21), are interpreted as oscillations of muon neutrinos into neutrinos that are not  $\nu_e$ 's, with a mass gap denoted by  $\Delta m_{23}^2$  (using the convention  $\Delta m_{ij}^2 \equiv m_j^2 - m_i^2$ ). The measured mixing angle  $\theta_{23}$  is close to maximal and  $|\Delta m_{23}^2|$  is in the range  $10^{-3}\text{--}10^{-2}$  eV<sup>2</sup>.
- Therefore, at least all three known neutrino families participate actively in the oscillations, leading to a  $3 \times 3$  neutrino-mixing matrix, as a minimum.
- In the likely limit  $\Delta m_{23}^2 \gg \Delta m_{12}^2$ , the solar and the atmospheric neutrino oscillations largely decouple and can effectively be described by the two-family oscillation formalism. Taking into account all three families, however, the solar-neutrino oscillation is governed by  $\theta_{12}$ ,  $\Delta m_{12}^2$  and  $\theta_{13}$ , while the atmospheric-neutrino oscillation is governed by  $\theta_{23}$ ,  $\Delta m_{23}^2$  and  $\theta_{13}$ . The two oscillation phenomena are linked through the angle  $\theta_{13}$ .
- If the LSND claim (22) of a transition  $\nu_\mu \rightarrow \nu_e$  with  $\Delta m^2 \sim 1$  eV<sup>2</sup> is correct, a fourth neutrino is needed which must be sterile since it is not seen in Z decay.

The open questions are, apart from the question of Dirac- or Majorana-type neutrinos, and accepting the phenomenon of neutrino oscillation as established:

- Is there a sterile neutrino?
- What are the values of the neutrino masses?
- What are the values of the mixing angles?
- Is there CP violation in the neutrino-mixing matrix?

## 5.2 *What will we learn within the next decade?*

From ongoing solar-neutrino experiments and from SuperKamiokande, but even more so from an impressive number of new experiments coming into operation within the next years (BOREXINO, ICANOE, KamLAND, K2K, MiniBooNe, MINOS, OPERA, and SNO), we may expect the following information:

- Neutrino oscillations will be ultimately confirmed, and sterile neutrinos will

be ruled out (ICANOE, MINOS, SNO, and SuperKamiokande/K2K: from the ratio of the flavour-blind neutral-current rate to the charged-current rate; ICANOE and OPERA: from the direct observation of  $\nu_\tau$  events; Mini-BooNE: direct check of the LSND claim).

- The atmospheric neutrino parameters will be known with better precision. Experimental information relevant for a more precise knowledge of the atmospheric neutrino fluxes will become available (23; 24). Also, forthcoming long-baseline accelerator experiments (CERN to Gran Sasso, Fermilab to Soudan) will improve the precision of  $|\Delta m_{23}^2|$  and  $\theta_{23}$ . For example,  $|\Delta m_{23}^2|$  is expected to be measured at MINOS with an accuracy better than 10% if  $|\Delta m_{23}^2| > 3 \times 10^{-3} \text{ eV}^2$  (25).
- It will be known which of the various sets of possible solar-neutrino oscillation parameters is correct (from all solar-neutrino experiments, including BOREXINO and KamLAND in their capacity as long-baseline reactor neutrino experiments).

Of course, the above is the conservative view. The LSND claim may actually be confirmed, with important consequences for cosmology. Or the Homestake solar-neutrino experiment, which claims a larger deficit of solar neutrinos than all other solar-neutrino experiments and has a large weight when the energy dependence of the deficit is exploited (and is largely responsible for the values of  $\Delta m_{12}^2$ ), may revise its results. In any such case, things would become even more interesting and would underline rather than undermine the physics case for the neutrino factory.

### 5.3 *What will be the questions in ten years from now?*

There is a strong case for going further in the fundamental quest of the neutrino masses and mixing angles, as a necessary step to unravelling the fundamental new scale(s) behind neutrino oscillations. However, in ten years from now no significant improvement can be expected in the knowledge of:

- The angle  $\theta_{13}$ , which is the link between the atmospheric and solar neutrino realms, for which the present CHOOZ bound is  $\sin^2 \theta_{13} \leq 5 \times 10^{-2}$  (26; 27). In forthcoming long-baseline experiments, only a minor improvement will be possible (27).
- The sign of  $\Delta m_{23}^2$ , which determines whether the three-family neutrino spectrum is of the ‘hierarchical’ or ‘degenerate’ type (i.e. only one heavy state and two almost degenerate light ones, or the reverse).
- Leptonic CP violation.
- Matter effects in the neutrino propagation through the Earth: a model-independent experimental confirmation of the MSW effect will not be available.

How would these questions be best addressed?

Both atmospheric and planetary experiments have an energy range such that  $\Delta m^2 L/E_\nu \ll 1$  for the smaller ( $\Delta m_{12}^2$ ) but not necessarily for the larger ( $\Delta m_{23}^2$ ) of these mass gaps. Even then, solar and atmospheric transitions are not (provided  $\theta_{13} \neq 0$ ) two separate two-family oscillations. For  $|\Delta m_{12}^2| \ll |\Delta m_{23}^2|$ , neutrino oscillation probabilities at planetary distances are well described by only three parameters,  $\theta_{23}$ ,  $\Delta m_{23}^2 = \Delta m_{13}^2$  and  $\theta_{13}$ :

$$\begin{aligned} P_{\text{CP}}(\nu_e \rightarrow \nu_\mu) &= \sin^2 \theta_{23} \sin^2 2\theta_{13} \sin^2 \left( \frac{\Delta m_{23}^2 L}{4E_\nu} \right), \\ P_{\text{CP}}(\nu_e \rightarrow \nu_\tau) &= \cos^2 \theta_{23} \sin^2 2\theta_{13} \sin^2 \left( \frac{\Delta m_{23}^2 L}{4E_\nu} \right), \\ P_{\text{CP}}(\nu_\mu \rightarrow \nu_\tau) &= \cos^4 \theta_{13} \sin^2 2\theta_{23} \sin^2 \left( \frac{\Delta m_{23}^2 L}{4E_\nu} \right). \end{aligned} \quad (1)$$

Equations (1) are indeed a very good approximation when the solar parameters lie in the SMA-MSW or VO range.

The present best fit value for  $\theta_{13}$  is in the range  $6^\circ$ – $8^\circ$  (28; 29), although it is compatible with zero within errors. Among the transitions in Eq. (1) the channels  $\nu_e \rightarrow \nu_\mu$  and  $\nu_e \rightarrow \nu_\tau$  have clearly the best sensitivity to a small  $\theta_{13}$ . From the experimental point of view, the measurement of  $\nu_e \rightarrow \nu_\mu$  oscillations through the appearance of wrong-sign muons is far superior to that of  $\nu_e \rightarrow \nu_\tau$  oscillations since the latter involves the detection of tau's. In Ref. (30), it was shown that the measurement of wrong-sign muons can improve the present limits on  $\theta_{13}$ , which are largely set by CHOOZ data (26), by at least two orders of magnitude.

As for CP violation, it is possible to construct a measurable CP-odd asymmetry, which in vacuum is proportional to  $\sin \delta$ . In Refs. (30) and (31), the authors considered the following integrated asymmetry (see also Ref. (32)):

$$\bar{A}_{e\mu}^{\text{CP}} = \frac{\{N[\mu^-]/N_o[e^-]\}_+ - \{N[\mu^+]/N_o[e^+]\}_-}{\{N[\mu^-]/N_o[e^-]\}_+ + \{N[\mu^+]/N_o[e^+]\}_-}. \quad (2)$$

The sign of the decaying muons is indicated by a subindex,  $N[\mu^+]$  ( $N[\mu^-]$ ) are the measured number of wrong-sign muons, and  $N_o[e^+]$  ( $N_o[e^-]$ ) are the expected number of  $\bar{\nu}_e$  ( $\nu_e$ ) charged-current interactions in the absence of oscillations. The significance of this asymmetry (i.e. the asymmetry divided by its statistical error) scales with the baseline and neutrino energy in the

following way:

$$\frac{\bar{A}^{\text{CP}}}{\delta \bar{A}^{\text{CP}}} \propto \sqrt{E_\nu} \left| \sin \left( \frac{\Delta m_{23}^2 L}{2} \right) \right|.$$

The best sensitivity to a non-zero CP-odd asymmetry is found at the maximum of the atmospheric oscillation. At the corresponding distance, however, matter effects are already important and must be taken into account.

Of all neutrino species, only  $\nu_e$  and  $\bar{\nu}_e$  have charged-current elastic scattering amplitudes on electrons. That induces effective ‘masses’  $\mu = \pm 2 E_\nu A$ , where the signs refer to  $\nu_e$  and  $\bar{\nu}_e$  and  $A$  is the matter parameter,

$$A = \sqrt{2} G_F n_e,$$

with  $n_e$  the ambient electron density (19).

Matter effects may be important if  $A$  is comparable to, or bigger than, the quantity  $\Delta_{ij}$  for some mass difference and neutrino energy, and if distances are large enough for the probabilities to be in the non-linear region of the oscillation. In the LMA-MSW solar scenario, and only in this scenario, the effects of  $\Delta m_{12}^2$  are not negligible over planetary distances. Matter effects induce an asymmetry between neutrino and antineutrino oscillation probabilities even in the absence of genuine CP violation.

For the Earth’s crust and outer mantle, with density  $\rho \sim 2.8 \text{ g/cm}^3$  and roughly equal numbers of protons, neutrons and electrons,  $A \sim 10^{-13} \text{ eV}$ . The typical neutrino energies under consideration are tens of GeV. For instance, for  $E_\nu = 30 \text{ GeV}$   $A \sim 1.1 \times 10^{-4} \text{ eV}^2/\text{GeV} \sim \Delta m_{23}^2$ . This means that matter effects will be important at long distances. Notice that at  $L = 732 \text{ km}$  and  $3500 \text{ km}$  the neutrino path remains in the Earth crust, whereas for  $7332 \text{ km}$  the flight path touches the denser mantle and  $A \sim 1.5 \times 10^{-4} \text{ eV}^2/\text{GeV}$ .

The method of choice to study these topics is to measure the transition probabilities of  $\nu_e(\bar{\nu}_e) \rightarrow \nu_\mu(\bar{\nu}_\mu)$ , currently perceived as the most important measurement at the neutrino factory.

The measurement of matter effects in oscillation experiments with very long baselines were discussed by Campanelli et al. (33), Freund et al. (34), and recently in comprehensive detail by Cervera et al. (35).

The neutrino factory is the best machine known today to address the above questions. When discussing the operation parameters of the neutrino factory, it seems obvious that these should not be driven by today’s physics questions

but in the first instance by the questions which will be asked in ten years from now.

## 6 Muon storage ring parameters

At this workshop, and in subsequent meetings of the oscillation physics working groups, agreement was found on several important machine parameters, which are recalled here.

Unanimously agreed is the machine's dual polarity, that is the ability to store both  $\mu^+$  and  $\mu^-$ , though never simultaneously so as not to spoil the concept of measuring 'wrong-sign muons'. It is not expected that the magnet polarity of the muon storage ring is switched more often than once every few months.

### 6.1 Number of injected muons per year

Ultimate sensitivity to the neutrino-mixing matrix parameters, in particular to  $\theta_{13}$  and  $\delta$ , requires a data set as large as possible.

The proposed number of injected muons per year ranges between  $10^{20}$  and  $10^{22}$ , the driver for the high end being leptonic CP violation. The largely accepted target figure is  $10^{21}$  injected muons per year. With one straight section comprising about 25% of the circumference of the muon storage ring, that gives a number of  $\sim 2.5 \times 10^{20}$  'useful' muon decays per year which serves as reference number often found in the recent literature.

To demonstrate how unprecedented these rates are, it is useful to note that MINOS expects to get  $10^{18}$  muon neutrinos and only  $5 \times 10^{15}$  electron neutrinos per year.

### 6.2 Muon momentum

The momentum of the circulating muons is in principle a free parameter. Thanks to the  $E_\mu^3$  dependence of the neutrino rates in the far detector, one always wins, background considerations aside, with higher momentum of the circulating muons, as shown in Fig. 5. Therefore, from the mere physics point of view, there is a strong incentive to run the neutrino factory at the highest possible muon momentum.

It has been argued that in case one wanted to avoid backgrounds from higher

energy neutrino events it might be useful to run at lower muon momentum. Given what energy is most sensitive to oscillations for a given distance and

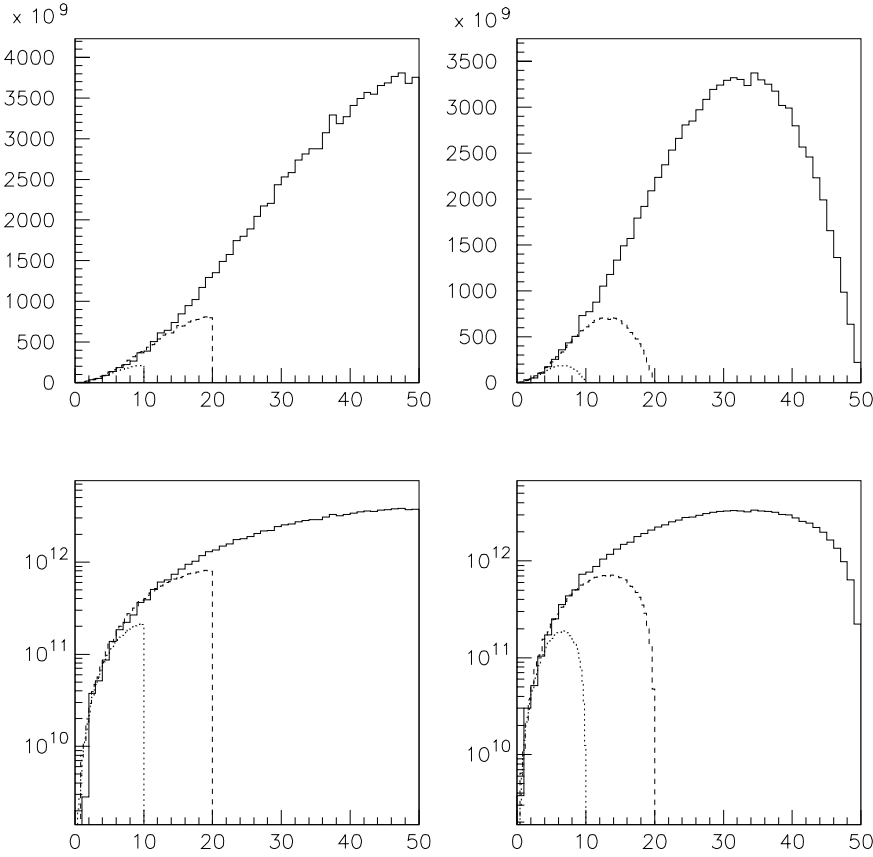


Fig. 5.  $\bar{\nu}_\mu$  and  $\nu_e$  fluxes (linear and logarithmic scales) produced by the decay of an ideal beam of  $\mu^+$  of  $E_\mu = 10, 20$  and  $50$  GeV/ $c$ .

$\Delta m^2$ , different neutrino energies imply different sources of background. For illustration, let us consider the observation of  $\nu_\mu \rightarrow \nu_\tau$  oscillations. At ‘low’ neutrino energy (10 GeV), there is negligible background from charm production. At ‘high’ neutrino energy (30 GeV)  $\nu_\tau$  appearance becomes easier since (i) the tau mass suppression will be smaller so more of them will be produced, and (ii) the tau will travel farther before it decays. Although background from charm production does become higher with energy, it is also more kinematically distinguishable from the signal and is ultimately less of a background.

Comparing data at the same value of  $L/E$ , albeit at different  $L$  and  $E$ , permits in principle to disentangle CP violation and matter effects. However, a 50 GeV/ $c$  muon momentum generates anyway a continuous neutrino energy

spectrum between zero and 50 GeV.

Altogether, no compelling physics reason to operate the neutrino factory at a lower than its maximum muon momentum has yet been found. Today's consensus is that 50 GeV/ $c$  muon momentum is a reasonable compromise between physics which wants as high a neutrino energy as possible, and the machine's cost which is a strong driver towards low muon momentum.

### 6.3 Muon beam divergence

For a 50 GeV/ $c$  unpolarized muon beam, half of all neutrinos are emitted in the forward direction within the cone subtended by the angle  $\theta = 1/(\beta\gamma) = m_\mu/p_\mu \sim 2$  mrad. In order not to disturb appreciably the flux per unit area at the location of the 'far' detector in the very forward direction, the flight path of the muons in the storage ring's straight section should have a divergence  $\sigma_\theta^\mu$  which is small compared with the natural cone angle of forward-going neutrinos, as argued by Papadopoulos (36), and Crisan and Geer (37).

For an additional angular divergence of the muon beam of  $0.1/(\beta\gamma)$ , the loss of flux at a detector at 1000 km distance would be  $\sim 2\%$ . For a muon-beam divergence less than  $0.05/(\beta\gamma)$ , there would be no appreciable loss of flux.

For a muon-beam divergence of  $0.1/(\beta\gamma)$ , the relative loss of flux is (37)

$$\frac{\Delta\Phi}{\Phi} \sim 0.03 \frac{\Delta\sigma_\theta^\mu}{\sigma_\theta^\mu}.$$

A 10% uncertainty in the muon-beam divergence would thus lead to a flux uncertainty of 0.3%.

Therefore, as a guideline for studies of the lattice of the muon storage ring's straight sections, an upper limit on the muon-beam divergence of less than  $0.1/(\beta\gamma)$  has been agreed between accelerator designers and particle physicists, and that the muon-beam divergence should be known to better than 10%.

A finite beam divergence together with finite polarization leads to a larger flux uncertainty, though. Further studies are needed to set realistic limits on the uncertainties of both muon-beam divergence and muon-beam polarization, with a view to keeping the resulting flux uncertainty well below 1%.

#### 6.4 *Geometric configuration of the storage ring*

At the early stage, the neutrino factory was imagined with a racetrack shape. However, this configuration is inefficient since it serves only one ‘far’ detector. Moreover, the neutrinos from the second leg of the racetrack exit to the surface only a few kilometres away from the neutrino factory. Estimations of the radiation hazard arising from the secondaries from neutrino interactions in the rock just before exiting to the surface show that the exit zone must be declared a ‘radiation zone’, with a radiation which is not large but is comparable to the legal limits of the radiation dose in publicly accessible areas (38; 39). Since the radiation problem is proportional to the intensity of stored muons, the racetrack design is disfavoured for a high-intensity neutrino factory.

As the storage ring costs only a fraction of the whole neutrino factory complex, one should try to optimize the number of ‘useful’ neutrinos per accelerated muon: those which come from muons that decay in the straight section pointing to the detector. The efficiency of a storage ring is higher, the longer the useful straight sections with respect to the circumference.

One obvious way to increase the efficiency of a storage ring is to orient the two long straight sections towards two different ‘far’ detectors. The inclinations of the straight sections define the distances to the detectors. Two different geometries exist which orient the two long straight sections to two detectors at different distances: the ‘bow-tie’ and the ‘triangle’. Although more difficult to build, the bow-tie is more efficient.

The other obvious way to increase the efficiency is to make the straight sections long compared with the circumference. This can be achieved by making the radius of the bending arcs as small as possible and by keeping the angle between the two straight sections as small as possible. The angle, however, is fixed by the directions to the two detectors.

Calculations (40) show that the efficiency varies between 48% and 74% for different geometric layouts which serve simultaneously two detectors at suitable locations on the planet. Depending on the geometry, the bow-tie is up to 20% more efficient than the triangle.

#### 6.5 *Neutrino beam parameters*

While the geometry and composition of the neutrino beams originating from a muon storage ring are far more useful for oscillation measurements than those of conventional beams, the uncertainties on the beams are also expected to be much smaller than those associated with conventional beams.

The momentum of the muon beam could be known from magnet current measurements to  $\sim 10^{-3}$  per fill, or one order of magnitude better than conventional neutrino experiments have known. If there is finite muon polarization and the spin precession frequency method can be employed, an even smaller uncertainty of the energy scale of the neutrino beam can be envisaged. The problem with precession-based measurements is, however, that they require a planar machine geometry with  $2\pi$  net bending as is the case in the ‘triangle’ configuration. They are not possible in a machine geometry with zero net bending as is the case in the ‘bow-tie’ configuration.

The beam current should be known with a precision of well below 1%, which would improve neutrino cross section measurements by more than one order of magnitude. The major problem there seems to be the background from decay electrons which contribute to the signal measured by current loops, a problem which deserves further study.

The time structure of the muon beam could also be used as a tool, in particular to reduce background from cosmic rays. Replenishment of the muons with a frequency between 10 and 100 Hz would permit that, as the effective muon lifetime is  $\sim 1$  ms. This replenishment cycle would also enable experiments to look for long-lived neutral particle decays. If there is also a  $\sim 100$  MHz fine-structure, experiments could try to exploit this, but given the expected size of the ‘far’ detectors, signals will arrive at times varying by several nanoseconds, rendering timing with 1 ns resolution a costly endeavour.

In oscillation experiments of the ‘disappearance’ type performed in conventional neutrino beams, a ‘near’ detector was mandatory to achieve high precision. This ‘near’ detector was built as identical in structure as possible to the ‘far’ detector, and was to compensate for the large uncertainty in the knowledge of the absolute flux, but also for the imprecise knowledge of the neutrino–nucleon cross-section. This concept of the ‘near’ detector has lost its significance at the neutrino factory. The absolute flux should be known at the neutrino factory with a precision better than 1%. The cross-section can and should be measured with a ‘near’ detector (which is free in optimizing its technology and internal structure, independently of any ‘far’ detector) with a comparable precision. The ratio of neutrino and antineutrino cross-sections, important for CP violation studies, should be measurable to an even better precision.

## 6.6 *Parameter summary*

The beam parameters that are available at a muon storage ring are appealing for both oscillation and ‘near’ detector measurements. The most important

parameters for oscillation measurements are the number of injected muons and the muon beam momentum, which should both be as high as possible. The baseline figures are  $10^{21}$  injected muons per year and 50 GeV/ $c$  momentum. That is not to say, however, that more conservative figures such as  $10^{20}$  injected muons per year and 20 GeV/ $c$  muon-beam momentum would not also permit interesting physics, an issue which deserves further study.

Evaluating the merits of other beam parameters is less straightforward. The time structure of the muon beams can serve as a way to reduce backgrounds from cosmic rays and allow more flexibility in detector design, but is not considered critical. Finally, especially in conjunction with a net polarization in the muon beam, it becomes important that the beam divergence be very small or well known.

Of course, if the additional effort to make two straight sections in the storage ring at different angles with respect to the horizontal is not prohibitive, one should certainly do so in order to take advantage of the considerable effort that has gone into the making of these intense muon beams.

To date, reasonable agreement on the experimentalist's desiderata on the parameters of the neutrino factory has been reached. It may read as follows:

- *Energy of circulating muons*  
The higher the better; default: 50 GeV/ $c$ .
- *Charge sign of circulating muons*  
Both signs needed; as far as possible the same intensity; no concurrence of both signs.
- *Injected muons per year*  
Baseline  $10^{21}$ ; upgradable to  $10^{22}$  or more.
- *Fraction of 'useful' decays*  
25% or larger.
- *Beam divergence in long straight sections*  
Less than  $0.1/(\beta\gamma) = 0.2$  mrad at 50 GeV/ $c$ , known to better than 10%.
- *Geometric configuration of the storage ring*  
'Triangle' or 'bow-tie'.

## 7 An appraisal of muon polarization

Muons from pion decay are 100% polarized in the pion rest frame. The average muon polarization in the laboratory frame is reduced to below 30% for pions above 250 MeV/ $c$  momentum. For a pion with given momentum, the muon polarization is correlated with the muon momentum. Therefore, the concept has been developed (11) to separate muons of different momentum in succes-

sive RF buckets, thus creating muon bunches with different polarization. After all beam gymnastics, muon-beam polarization in the storage ring at the level of 30% and perhaps even more might be possible (13).

If one wants to preserve longitudinal polarization using  $g - 2$  precession in the muon storage ring, certain beam momenta are required, namely 22.656 GeV/ $c$  or 45.311 GeV/ $c$ .

One example of where a well-measured polarization could be useful is if one saw an excess of electron-like events in a ‘far’ detector, but there was no electron charge identification. By varying the beam polarization one changes the relative strength of the muon and electron neutrino components of the beam, and can thus determine whether, for example, electron-like events came from  $\nu_\mu$ ’s or  $\bar{\nu}_e$ ’s. This elegant feature of the neutrino factory is diluted, however, if the muon-beam divergence is non-zero.

More generally, one can ask for which physics case polarization is vital. From the point of view of ‘switching off’ events from the electron neutrino content of the initial beam, the study of all oscillations  $\nu_e \rightarrow \nu_\mu$  and  $\nu_e \rightarrow \nu_\tau$  will hardly want the wrong polarization. On the contrary, the increase of the electron neutrino flux with the right polarization may well be wanted. This is in particular the case for the channel  $\nu_e \rightarrow \nu_\mu$  which is experimentally most easily accessible, through the observation of ‘wrong-sign’ muon events, with high precision. The study of the channels  $\nu_\mu \rightarrow \nu_e$  and  $\nu_\mu \rightarrow \nu_\tau$  is likely to profit from muon polarization by the reduction of background from events originating from the electron neutrino component of the beam.

The assessment of muon polarization deserves further, quantitative, study.

Whatever the polarization of the circulating muons, knowing it is of prime importance because the neutrino spectral shape depends critically on the degree of polarization as discussed earlier in Section 4. Fortunately, the measurement (which exploits the  $g - 2$  spin precession in the muon storage ring, measuring the oscillation amplitude, the oscillation frequency and the decrease with time of the oscillation amplitude) is in principle straightforward through the measurement of the energy of the decay electrons at a given angle with respect to the muon momentum. A possible scheme to measure the muon polarization, together with the muon momentum and the energy spread of the muon beam, has been worked out by Blondel (41).

## 8 Detector concepts for long-baseline experiments

Ideally, one would like to study all transitions listed in Table 4 together with the transitions of the respective antiparticles.

Table 4

Neutrino flavour transitions.

	$\nu_e$ beam	$\nu_\mu$ beam	$\nu_\tau$ beam
Appearance	$\nu_e \rightarrow \nu_\mu$	$\nu_\mu \rightarrow \nu_e$	$\nu_\tau \rightarrow \nu_e$
Appearance	$\nu_e \rightarrow \nu_\tau$	$\nu_\mu \rightarrow \nu_\tau$	$\nu_\tau \rightarrow \nu_\mu$
Disappearance	$\nu_e \rightarrow \nu_x$	$\nu_\mu \rightarrow \nu_x$	$\nu_\tau \rightarrow \nu_x$

The neutrino factory adds significantly to the possibilities through the novel feature of a well-defined  $\nu_e$  beam. A  $\nu_\tau$  beam is not within reach, however — neglecting possible T-violation effects — all channels accessible with a  $\nu_\tau$  beam are also accessible with the  $\nu_e$  and  $\nu_\mu$  beams of the neutrino factory.

We note that in principle three types of detector are called for: one for tau detection, one for electron and one for muon detection, always including the separation of the charge of the respective lepton, which distinguishes the interactions of neutrinos from those of antineutrinos.

Ideally, for both a ‘near’ and ‘far’ detector, one would want to build something that could do particle identification and charge measurements for all three families of charged leptons. Muons are the easiest to identify, taus are the next easiest if only because of their decay to muons, and finally electrons are the most difficult. Although detector technologies exist that could achieve all these goals, the challenge lies in making such a detector with a mass of tens of kilotons, without exhausting the world’s high-energy physics budget.

In practice, tau detection poses stringent requirements on the detector. One established way is to track the decay kink of the charged tau through precise track-coordinate measurement in emulsions. However, unlike the case of the conventional  $\nu_\mu$  beam from  $\pi^+$  and  $K^+$  decay, there is in the neutrino factory an equal-strength  $\bar{\nu}_e$  component in the beam which worsens significantly the background arising from charmed particle decays.

If by the time that the neutrino factory is in operation we still believe that oscillations are occurring between  $\nu_\mu$  and  $\nu_\tau$ , but  $\tau$ ’s have not been observed in long-baseline neutrino experiments, then one detector at the neutrino factory will emphasize  $\nu_\tau$  appearance. Technically, that can be done either through observing the tau-decay kink in emulsions (OPERA-like as described by Strolin (42)),

suitably modified for the operation with the much higher event rate at the neutrino factory, or according to a new concept employing magnetized iron sheets between emulsion sheets as proposed by Harris and Para (43)), or by kinematical selection (ICANOE-like, as described by Campanelli (44)).

Another detector-type would look for electrons from the interaction of electron neutrinos, albeit without charge discrimination since no easy and financially affordable recipe exists for achieving that in detectors with a mass of tens of kilotons. Naturally, one is led to think of SuperKamiokande or a an even bigger successor employing the observation of Cherenkov light in water.

But from the arguments given in Section 5, the physics emphasis is likely on measurements of the oscillations  $\nu_e \rightarrow \nu_\mu$  and  $\bar{\nu}_e \rightarrow \bar{\nu}_\mu$ , which would only require muon identification, energy, and muon charge measurements.

The discussion of suitable detectors for the neutrino factory naturally touches on (i) the potential of detectors which are expected to be built within the next years to exploit the long-baseline beams from CERN to Gran Sasso, and from Fermilab to Soudan, and (ii) the potential of new detectors conceived and optimized for the beams of the neutrino factory.

### 8.1 Detectors for $\nu_\tau$ detection

Special technologies must be employed to achieve electron or tau identification event-by-event, or electron or tau charge measurements. For the neutrino factory, these technologies will be considered a priority issue only if no  $\nu_\tau$  appearance will have been observed at the planned long-baseline experiments in the CERN NGS beam.

One category of new detectors which builds on the CHORUS experience and OPERA design, would typically use thin ( $\sim 100 \mu\text{m}$ ) sheets of emulsion combined with low-density ( $\sim 300 \mu\text{m}$ ) spacers, so that one can measure kinks that occur when a tau decays, by comparing the slope of a track before and after the spacer. A detector combining thin sheets of emulsion with spacers and lead, would quickly develop the electromagnetic showers. This would be very useful for identifying taus, and electrons, but not for measuring their charges. Therefore, one might also imagine constructing an emulsion/magnetized steel calorimeter (43), where again there were thin sheets of emulsion separated by spacers, but the target mass would be made up of thin sheets (0.1 cm) of magnetized steel. By comparing the change in slope between a few hundred of these sheets, one could make a  $4\sigma$  event-by-event measurement on electron or tau charge. This would have the tremendous advantage of knowing which of the initial neutrino type gave rise to the oscillation. The additional challenge in this design would be the creation of a large magnetic field in such a thin

yet large piece of steel. In general, making such detectors on the 10 kt scale would probably be prohibitively expensive, and not the way to make precision measurements of the oscillation parameters.

The OPERA concept of replacing ‘bricks’ after each interaction would not work without major modification, because of the many interactions expected at a neutrino factory (a factor of 100 more than in the CERN NGS beam), which would require too many exchanges and would be too costly (45).

Another category of new detectors which hold more promise for use on the 10 kt scale can be classified as detectors with ‘kinematic separation’. These detectors identify  $\tau \rightarrow \mu$  decays by their difference in kinematics, although they don’t see the kink from the decay itself. ICANOE (14), which uses a liquid argon TPC detector for the detection of  $\nu_\tau$ ’s, has the necessary charged track resolution to measure the acoplanarity of an event and determine the likelihood of it being a  $\nu_\tau$  interaction.

## 8.2 Large magnetic detectors

ICANOE, which came into being from a merger between ICARUS, the promoter of the liquid argon TPC, and NOE, the promoter of a magnetized-iron muon spectrometer, has interesting capabilities for the detection of wrong-sign muons in the muon spectrometer part, while being ultrasensitive to details at the interaction vertex when it lies inside the fiducial volume of the TPC, as emphasized by Cline (14).

A nice aspect of neutrino experiments is that one can put one right after the other and the beam is not attenuated. So it is straightforward to assume that a magnetized steel/scintillator sampling calorimeter would be one of the ‘far’ detectors at the neutrino factory. Depending on the geometry of such a detector, it might also prove useful as an atmospheric neutrino detector, although by then the atmospheric measurements available from SuperKamiokande and MINOS may well have exhausted that neutrino source as explained by Edgecock (46) and Litchfield (47).

To be quantitative, we consider a large magnetic detector of the type proposed by Cervera et al. (48). It has a cylindrical shape, 10 m radius and 20 m length, and is made of 6 cm thick iron rods interspersed with 2 cm thick scintillators segmented along their length. Its fiducial mass is 40 kT. A superconducting coil generates a solenoidal magnetic field of 1 T. A neutrino travelling through the detector sees a sandwich of iron and scintillator. The spatial coordinates of an event are measured from the location of the scintillator rods and by virtue of their longitudinal segmentation (light readout at both ends of each segment). A Monte Carlo simulation has been performed to quantify the response of the

detector.

In a  $\bar{\nu}_\mu, \nu_e$  neutrino beam from the decay of  $\mu^+$  of 50 GeV/c, the bulk of events in the detector are  $\bar{\nu}_\mu$  CC events signalled by the presence of a positive primary muon,  $\bar{\nu}_\mu$  and  $\nu_e$  NC events with no primary charged lepton, and  $\nu_e$  CC events for which the electron is not identified, though. The signal consists of ‘wrong-sign’  $\mu^-$  arising from the  $\nu_\mu$  produced by the oscillation  $\nu_e \rightarrow \nu_\mu$ .

Potential backgrounds to the wrong-sign  $\mu^-$  events are:

- $\bar{\nu}_\mu$  CC events in which the positive muon is not detected and a secondary negative muon arising from the decay of  $\pi^-, K^-$  and  $D^-$  hadrons fakes the signal. The most dangerous events are those with  $D^- \rightarrow \mu^-$ , which yield an energetic muon with a spectrum similar to the signal’s.
- $\nu_e$  CC events for which it is assumed that the primary electron is not detected. Charm production is not relevant for this type of event since the charmed hadrons in the hadronic jet have predominantly positive charge. Instead, the fake  $\mu^-$ ’s arise predominantly from the decay of negative pions in the hadronic jet.
- $\bar{\nu}_\mu$  and  $\nu_e$  NC events. Fake  $\mu^-$ ’s arise in this case also predominantly from the decay of negative pions and kaons, since associated-charm production is suppressed with respect to single-charm production in CC events.

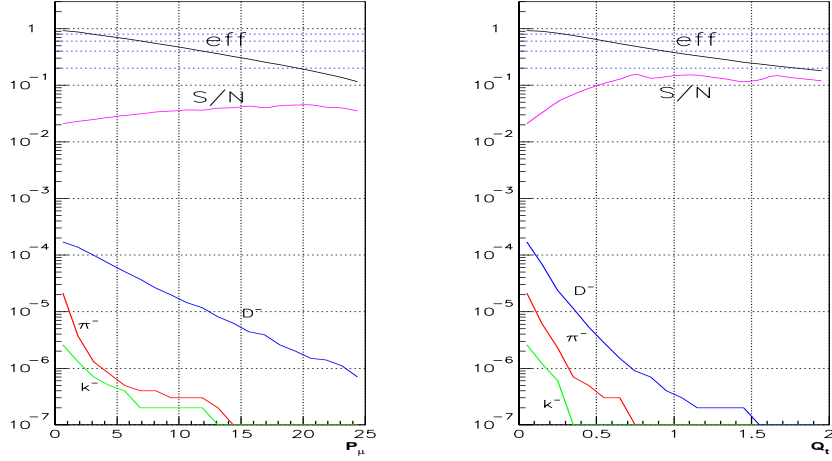
Although these backgrounds are large, simple kinematical cuts suppress them efficiently: for signal events the  $\mu^-$  candidate is harder and more isolated from the hadronic jet than for background events. An analysis is performed in two variables: the momentum of the muon,  $p_\mu$ , and the muon transverse momentum with respect to the hadron shower axis,  $q_t = p_\mu \sin \theta$ .

Figure 6 shows the efficiency for signal detection and the fractional backgrounds from  $\bar{\nu}_\mu$  CC and NC events, as a function of  $p_\mu$  and  $q_t$ . Also shown is the ratio  $S/N = \epsilon_s/\sigma_b$ , where  $\epsilon_s$  is the signal selection efficiency and  $\sigma_b$  is the error in the number of background events surviving the cuts. Muons from charmed-particle decays constitute the main background from  $\bar{\nu}_\mu$  CC events, while muons from pion decay dominate the backgrounds from NC events.

Figure 6 shows that the  $S/N$  ratio rises with  $p_\mu$  and  $q_t$ , and tends to saturate for  $p_\mu > 5 \text{ GeV}/c$  and  $q_t > 0.5 \text{ GeV}/c$ . Cutting at  $p_\mu > 7.5 \text{ GeV}/c$  and  $q_t > 1.0 \text{ GeV}/c$  maximizes the  $S/N$  ratio. Table 5 shows the signal efficiency and the fractional background contamination, while Table 6 shows the signal and background events, after cuts, for three different baselines.

The residual backgrounds are still rather high ( $\sim 10^2$ ) at ‘short’ distances (732 km), and become negligible only at distances of, and larger than, 3500 km. On the other hand, the oscillated signal at 3500 km is still as large as at 732 km (since the quadratic decrease in the flux is compensated by the increase in

### Charged-current events



### Neutral-current events

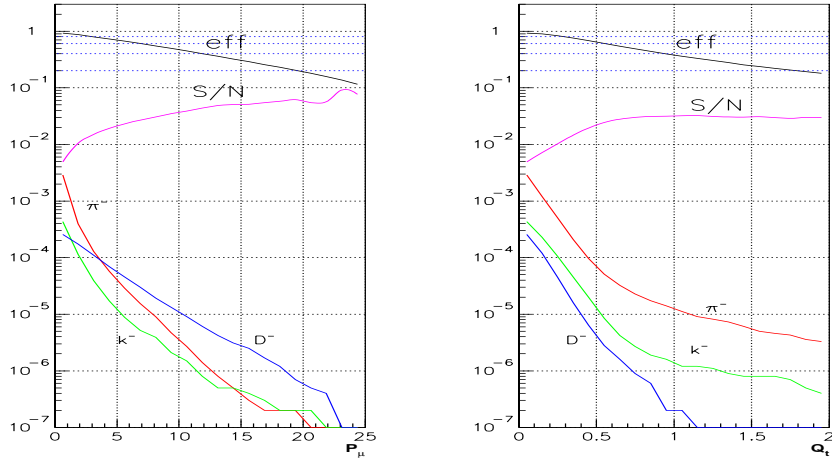


Fig. 6. Wrong-sign muon efficiency and fractional backgrounds from  $\bar{\nu}_\mu$  CC and NC events, in a neutrino beam originating from  $50 \text{ GeV}/c \mu^+$ .

oscillation probability) while it is smaller at very large distances (7332 km). Thus, the ‘intermediate distance’, ( $\sim 3500 \text{ km}$ ), turns out to be the best baseline from the point of view of optimizing the  $S/N$  ratio and thus the sensitivity to the oscillation parameters.

The large magnetic detector would be adequate for measurements of  $\theta_{13}$  and the CP-violating phase  $\delta$ , both of which would contribute significantly to the field.

Table 5

Signal efficiency and fractional backgrounds for the wrong sign muon search with  $\mu^+$  decays.

$\nu_\mu$ (signal)	$\bar{\nu}_\mu$ CC	$\nu_e$ CC	$\bar{\nu}_\mu + \nu_e$ NC
$3 \times 10^{-1}$	$1.0 \times 10^{-7}$	$5.0 \times 10^{-7}$	$1.0 \times 10^{-6}$

Table 6

Events surviving the cuts in the large magnetic detector for  $10^{21}$  useful  $\mu^+$  decays. The signal events have been calculated with the parameters  $\Delta m_{23}^2 = 4 \times 10^{-3} \text{ eV}^2$ ,  $\theta_{12} = 45^\circ$  and  $\theta_{13} = 13^\circ$ .

Baseline (km)	$\nu_\mu$ (signal)	$\bar{\nu}_\mu$ CC	$\nu_e$ CC	$\bar{\nu}_\mu + \nu_e$ NC
732	$3.3 \times 10^4$	3.5	30	31
3500	$3 \times 10^4$	$\sim 0.1$	1.2	1.2
7332	$1.3 \times 10^4$	$< 0.1$	$< 0.2$	$< 0.2$

### 8.3 Deep underground ‘far’ detector location?

For multi-kiloton ‘far’ detectors, the surface is naturally large, several hundred square metres. Accordingly, the number of cosmic-ray muons which traverse the detectors is huge if they are not located deep underground: several  $10^4$  muons per second. This is to be compared with the number of atmospheric neutrino events,  $10^{-4}$  per second, and the number of events expected from a neutrino factory, for example at a distance of 732 km with  $10^{21}$  useful 50 GeV/ $c$   $\mu^+$  decays per year, that is  $10^{-2}$  events per second.

The question is how much background the cosmic muons create to neutrino events, and even more so to the sub-sample of ‘interesting’ neutrino events such as ‘wrong-sign’ muon events. There is no general answer to this question since it depends on the design of the detector. However, in order to highlight the problem, an order of magnitude estimate may be in order.

The effect of the cosmic muons can be reduced by veto planes but only by two to three orders of magnitude. One more order of magnitude may be gained by timing coincidence with the replenishment cycles of the neutrino factory. These reductions are insufficient. An effective method to reduce further the background from cosmic muons is by location deep underground, which can add three or more orders of magnitude depending on the amount of overburden by rock. Thus, an appropriate design together with an underground location at sufficient depth may lead to only one cosmic-muon background event per

neutrino event from the neutrino factory.

Therefore, the location of a ‘far’ detector seems much constrained not only by the necessity for a convenient surface location, but also by the availability of a suitably equipped deep underground laboratory.

## 9 Physics reach of long-baseline oscillation experiments

We consider first the potential of a  $\nu_\tau$ -appearance detector employing the emulsion technique. Table 7 gives approximate numbers for the comparison between the situation at the neutrino factory and the ‘optimized’ NGS beam (9) from CERN to Gran Sasso. One year of operation with a 1 kt target and  $4.5 \times 10^{19}$  400 GeV/ $c$  protons on target at the NGS is compared to one year of operation with a 1 kt target and  $10^{21}$  injected 50 GeV/ $c$  muons at a distance of 732 km from the neutrino factory. In the latter case, the increased background from charm production is estimated (42) according to

$$N_{\text{charm}} \sim 3 \times 10^{-5} N_{\text{CC}}(\nu_\mu) + 3 \times 10^{-4} N_{\text{CC}}(\bar{\nu}_e).$$

Table 7

$\nu_\tau$  detection with an emulsion detector suitably modeled after OPERA, in the optimized NGS and at the neutrino factory. The oscillation  $\nu_\mu \rightarrow \nu_\tau$  is assumed to take place with  $\sin^2 2\theta = 1$  and  $\Delta m^2 = 3 \times 10^{-3} \text{ eV}^2$ .

	$\nu_\mu$ CC events	$\nu_\tau$ CC events	Background events
NGS	2450	21.4	0.07
Neutrino factory	$2.5 \times 10^5$	2140	44

While the  $\nu_\tau$ -appearance experiment employing the emulsion technique would still give an interestingly large number of events above background, it will probably no longer be of interest when the neutrino factory comes into operation because of the limited number of events in an emulsion target.

Considerably more  $\nu_\tau$  events, albeit with more background contamination, could be produced in an ICANOE-like detector (14; 44) which would employ a kinematic selection of  $\nu_\tau$  interactions à la NOMAD. The physics reach of that line of work is still to be worked out.

Other detector types concern the identification and measurement of final-state electrons and muons. This is considerably easier for muons than for electrons, yet detectors might be contemplated which can do a good job for both electrons and muons, for instance again along the lines of the ICANOE

design. However, we may again expect that at the time the neutrino factory comes into operation, the standard measurements such as spectral distortions due to disappearance of  $\nu_e$  or  $\nu_\mu$ , or abnormal ratios of ‘short’ to ‘long’ events in calorimetric detectors, will no longer be in the focus of interest.

That leaves the physics reach of ‘wrong-sign’ muon detection, be it in an ICANOE-like detector (14; 33; 44) or in a dedicated large magnetic detector.

A detailed analysis of the physics reach in a dedicated large magnetic detector has been made by Cervera et al. (35). It includes a study of the dependence of the signal as function of neutrino energy, and reveals that a baseline of about 3500 km is a pretty good choice. The comparison of the number of wrong-sign muons detected running in the two polarities and the binning in energy of the signal are strong analysis tools to disentangle  $\theta_{13}$  and  $\delta$  at such a baseline. This optimal distance is in nice agreement with earlier studies based on the significance of integrated asymmetries (30; 31; 49), as demonstrated in Fig. 7.

A decisive conclusion is that baselines much larger than 732 km are needed, for the following reasons:

- In the SMA-MSW or VO scenarios, the sign of  $\Delta m_{23}^2$  can only be determined for distances where matter effects are sizeable and the CP asymmetries they induce are measurable. This happens at  $L = O(3000)$  km or larger.
- In the LMA-MSW scenario, there is a strong correlation between  $\theta_{13}$  and  $\delta$  at short distances. It is necessary to go far away so that the different energy dependence shows up and the signals in the CP-conjugate channels differ sizeably, which permits the simultaneous measurement of both parameters.

Quantitatively, two-parameter fits at a baseline of 3500 km give the following results (35):

- The angle  $\theta_{13}$  can be measured with a precision of tenths of degrees, down to values of  $\theta_{13} = 1^\circ$ . Thus the sensitivity to  $\sin^2 \theta_{13}$  may be improved by three orders of magnitude or more.
- If the solar deficit corresponds to solar parameters in the LMA-MSW range, CP-violation may be within reach. The phase  $\delta$  can be determined with a precision of tens of degrees, for the central values allowed for  $|\Delta m_{12}^2|$ , and maximal CP violation can be disentangled from no CP violation at 99% CL for values of  $|\Delta m_{12}^2| > 2 \times 10^{-5} \text{ eV}^2$ .
- The sign of the atmospheric mass difference,  $\Delta m_{23}^2$ , can be determined at 99% CL, for  $\theta_{13}$  within the range  $\theta_{13} = 1\text{--}10^\circ$  and  $|\Delta m_{23}^2|$  in the range allowed by SuperKamiokande data.
- A model-independent confirmation of the MSW effect will be feasible, and the matter parameter  $A$  measured with a 10% precision, or better if combined with a very long baseline.

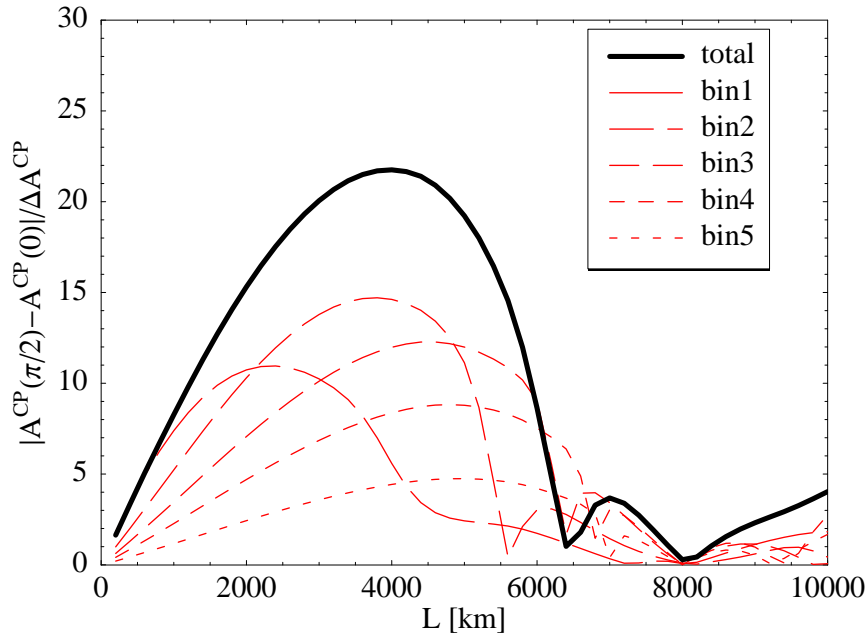


Fig. 7. The signal-over-noise ratio of the CP-odd asymmetry of Eq. 2 as a function of the distance, after subtracting the fake matter induced asymmetry. The thick line corresponds to the spectrum-integrated asymmetry, while the dashed lines correspond to the asymmetry computed in five energy bins of equal width  $\Delta E_\nu = 10$  GeV. The neutrino-mixing parameters correspond to the LMA-MSW solution to the solar anomaly:  $\Delta m_{23}^2 = 2.8 \times 10^{-3}$  eV<sup>2</sup>,  $\Delta m_{12}^2 = 1 \times 10^{-4}$  eV<sup>2</sup>,  $\theta_{12} = 22.5^\circ$ ,  $\theta_{23} = 45^\circ$ ,  $\theta_{13} = 13^\circ$  and  $\delta = 90^\circ$ . The muon momentum is  $E_\mu = 50$  GeV/ $c$  and the matter parameter  $A$  is varied with the distance according to Ref. (50).

In the case of the LMA-MSW solution, the combination of the two longest baselines may be useful if a multiparameter fit becomes necessary.

## 10 Near-detector neutrino physics opportunities

The advent of a muon storage ring would not only bring about new oscillation measurements that look pretty daring today, but would also usher in a new era of high-precision neutrino scattering experiments with a wide physics scope, as pointed out convincingly by de Jong (51), McFarland (52) and King (53). To highlight the main point: for a detector which is located 30 m from the end of a 150 m long straight section of a 50 GeV/ $c$  muon storage ring, for  $10^{21}$  injected muons per year, the event rate is 40 million events per kilogram per year over a 10 cm radius.

For oscillation-related measurements, one would focus on measuring the total neutrino and antineutrino cross-sections at low energies, as well as the beam divergence.

A necessary ingredient for measuring CP-violation effects is a precise knowledge of the ratio of neutrino–nucleon to antineutrino–nucleon cross sections which are poorly known especially at low energy as pointed out by Perez (54).

The absolute neutrino–nucleon cross-section is also one of three obstacles to a precise determination of the absolute flux of atmospheric neutrinos (the other two problems being the absolute flux of cosmic protons and helium nuclei, and significant uncertainties in the production of secondary pions in the interaction of the primary particles with nitrogen and oxygen nuclei). A precise flux of atmospheric neutrinos will be much in demand, because underground detectors exploiting the neutrino beam from a neutrino factory might also be excellent detectors for atmospheric neutrinos.

Therefore, one expects that the precision measurement of neutrino–nucleon cross-sections will be a major issue for ‘near’ detectors at the neutrino factory.

However, neutrinos could also be used as precision probes of nucleon structure much like electrons and muons have been used in the past. The new handle neutrinos provide is that they can measure the nuclear dependence of the valence and sea quarks as well as valence versus sea measurements of the spin distributions, using a polarized target (much like the SMC experiment at CERN did).

Another way to take advantage of the high neutrino fluxes would be to use this facility as a charm factory. Charged-current charm production from muon neutrinos provides a gold-plated signature when the charmed meson decays to a final-state muon with opposite-sign charge. For the same beam parameters stated above, there would be  $10^6$  leptonic tagged charm decays in a 4 kg·years exposure. With that kind of statistics one could consider measuring  $D^0 - \bar{D}^0$  mixing and  $V_{cd}$  order(s) of magnitude better than what is currently known.

Yet another possibility for new measurements with a ‘near’ detector in a neutrino beam from 50 GeV/ $c$  (or lower) muons would be a measurement of  $\sin^2 \theta_W$  from neutrino-electron scattering. This measurement, with an exposure of 250 kg·years, could yield a measurement of  $\sin^2 \theta_W$  with an uncertainty of  $\sim 1 \times 10^{-4}$ , which is a factor of 20 better than the current best measurement from deep inelastic neutrino–nucleon scattering, and comparable to the LEP measurement precision. The latter measurement is made in the time-like region of  $e^+e^-$  annihilation, though.

Still another aspect that should be taken into account, is that currently there are many physicists involved in nucleon structure measurements (primarily at

HERA) which will have been completed at the time that the neutrino factory comes into operation. Although most of these physicists are not involved with neutrino physics, when a muon storage ring becomes the ideal place to further their measurements they are likely to bring their support and expertise.

## 11 Further physics opportunities

The discovery of neutrino oscillations which require a non-zero neutrino mass and hence point to physics beyond the Standard Model, fuelled the interest in searches for rare phenomena which are strongly suppressed within the Standard Model. One such area is lepton flavour violation which is put in ‘by hand’ with the assumption of zero neutrino mass. SUSY models in particular predict branching ratios arising from radiative corrections which are within the reach of the next generation of experiments (55).

The neutrino factory is an abundant source of muons, also of low-momentum muons which are produced at the primary proton target in the backward direction and which could be captured and stopped, enabling a stopped-muon source of much higher intensity than used today, and therefore giving access to even lower branching ratios of very rare muon processes. The improvement of the rate of stopped muons over the rate at PSI is estimated at a factor of  $\sim 10^3$ .

Lepton-flavour-violating processes involving muons are

- $\mu^+ \rightarrow e^+ \gamma$ ,
- $\mu^- N \rightarrow e^- N$  conversion in nuclei,
- $\mu^+ \rightarrow e^+ e^+ e^-$ , and
- muonium–antimuonium conversion  $\mu^+ e^- \rightarrow \mu^- e^+$ .

The rare decay  $\mu^+ \rightarrow e^+ \gamma$  has been shown to be absent at the  $10^{-12}$  level. A new experiment with a sensitivity up to  $10^{-14}$  is under way at the PSI. The  $\mu^- N \rightarrow e^- N$  conversion in nuclei is measured to be absent at the level of  $10^{-12}$ , and a new experiment (MECO) at the BNL-AGS aims at improving this sensitivity to  $10^{-16}$ .

Studies of the potential of the neutrino factory in this area are still in their infancy. One major stumbling block to be overcome is the relatively low frequency of muon replenishment at the neutrino factory which is typically between 10 and 100 Hz. However, for ultrasensitive searches for rare phenomena a DC operation is much preferred.

## 12 Summary

Taking everything together, the physics potential of the neutrino factory looks very good. Even from a conservative perspective of the neutrino mixing matrix, the specific features of the muon beams originating from muon decay make possible experiments which are not feasible with conventional neutrino beams from pion and kaon decay. Outstanding issues are the high-precision measurement of  $\theta_{13}$  and CP violation studies, both in transitions of  $\nu_e \rightarrow \nu_\mu$ . The precise determination of CKM matrix elements of neutrino mixing will help us to understand what connects quarks and leptons. CP violation may be studied in neutrino oscillations in the cleanest way since it is not affected by hadronic uncertainties.

Yet Nature must be kind to have chosen the right set of solar neutrino oscillation parameters to make CP violation experimentally accessible. Ongoing as well as new experiments will tell within the next five years or so what the situation is, possibly making the case for the neutrino factory irresistibly strong.

However, if, for example, LSND is right, or Homestake is wrong and solar neutrinos are at a higher  $\Delta m^2$  than widely believed at present, and/or there are sterile neutrinos, then the neutrino oscillation programme at a muon storage ring will be far broader than outlined above.

A survey of ‘near’ detector measurements shows that this facility could also be the home of new dimensions in our understanding of nucleon structure.

Technically, the neutrino factory could be in operation within one decade or so. However, in the real world of scarce resources, political and financial considerations are more likely to determine the time schedule than technical factors.

## References

- [1] G.I. Budker, Proc. 7th Int. Conf. on High Energy Accelerators (Yerevan, 1969), p. 33; AIP Conf. Proc. **352** (1996) 4.
- [2] A.N. Skrinsky, Proc. Int. Seminar on Prospects of High Energy Physics (Morges, 1971); AIP Conf. Proc. **352** (1996) 6.
- [3] D.G. Koshkarev, CERN internal report CERN/ISR-DI/74-62 (1974).
- [4] Private communication from S. Wojcicki.
- [5] C.M. Ankenbrandt et al. (Muon Collider Collaboration), Phys. Rev. ST Accel. Beams **2** (1999) 081001;  
S. Geer, C. Johnstone and D. Neuffer, FERMILAB-PUB-99-121.

- [6] S. Geer, Phys. Rev. **D57** (1998) 6989; and erratum.
- [7] S. Geer and R. Raja (eds.), Proc. of the Workshop on physics at the first muon collider and front-end of a muon collider, AIP Conf. Proc. **435** (1998).
- [8] B. Autin, A. Blondel and J. Ellis (eds.), Prospective study of muon storage rings at CERN, Report CERN 99-02 (1999) and ECFA 99-197.
- [9] G. Acquistapace et al., The CERN neutrino beam to Gran Sasso (NGS), Report CERN 98-02 and INFN/AE-98/05; Addendum CERN SL-99-034 DI and INFN/AE-99/05.
- [10] V. Palladino, Neutrino beams from pion/kaon and muon decay: a comparison, these proceedings.
- [11] R. Palmer, C. Johnson and E. Keil, A cost-effective design for a neutrino factory, these proceedings.
- [12] See for example: T.K. Gaisser, Cosmic Rays and Particle Physics, Cambridge University Press, 1990.
- [13] A. Blondel, Muon polarisation in the neutrino factory, these proceedings.
- [14] D.B. Cline, Wrong-sign muon appearance with an ICARUS-like detector at a neutrino factory, these proceedings.
- [15] Y. Fukuda et al. (SuperKamiokande Collaboration), Phys. Lett. **B433** (1998) 9; Phys. Lett. **B436** (1998) 33; Phys. Rev. Lett. **81** (1998) 1562; Phys. Rev. Lett. **82** (1999) 2644; Phys. Lett. **B467** (1999) 185; T. Kajita (SuperKamiokande Collaboration), Nucl. Phys. **B77** (1999) 123.
- [16] S. Hatakeyama et al. (SuperKamiokande Collaboration), Phys. Rev. Lett. **81** (1998) 2016; E. Peterson (Soudan2 Collaboration), Nucl. Phys. **B77** (1999) 111; W.W. Allison, Phys. Lett. **B449** (1999) 137; F. Ronga et al. (MACRO Collaboration), Nucl. Phys. **B77** (1999) 117.
- [17] R. Davis et al. (Homestake Collaboration), Phys. Rev. Lett. **20** (1968) 1205; B.T. Cleveland et al., Astrophys. J. **496** (1998) 505; K. Lande et al., Nucl. Phys. **B77** (1999) 13; T. Kirsten, Nucl. Phys. **B77** (1999) 26; Y. Fukuda et al. (Kamiokande Collaboration), Phys. Rev. Lett. **77** (1996) 1683; Dzh.N. Abdurashistov et al. (SAGE Collaboration), Nucl. Phys. **B77** (1999) 20; Y. Fukuda et al. (SuperKamiokande Collaboration), Phys. Rev. Lett. **82** (1999) 1810; M. Smy et al., preprint hep-ex/9903034.
- [18] B. Pontecorvo, J. Expt. Theor. Phys. **33** (1957) 549; J. Expt. Theor. Phys. **34** (1958) 247; Sov. Phys. JETP **26** (1968) 984.
- [19] L. Wolfenstein, Phys. Rev. **D17** (1978) 2369; Phys. Rev. **D20** (1979) 2634; S. P. Mikheyev and A. Yu. Smirnov, Sov. J. Nucl. Phys. **42** (1986) 913.

- [20] Z. Maki, M. Nakagawa and S. Sakata, Prog. Theor. Phys. **28** (1962) 970; Particle Data Group, Review of Particle Physics, Eur. Phys. J. **C3** (1998) 1 (The convention for the sign of  $\delta$  used in the text is opposite to the one used in this reference).
- [21] Y. Hayato, SuperKamiokande: status and perspectives, these proceedings.
- [22] C. Athanassopoulos et al. (LSND Collaboration), Phys. Rev. Lett. **81** (1998) 1774; Phys. Rev. **C58** (1998) 2489.
- [23] M. G. Catanesi et al. (HARP Collaboration), Proposal to study hadron production for the neutrino factory and for the atmospheric neutrino flux, CERN-SPC-99-35 (1999).
- [24] J. Alcaraz et al. (AMS Collaboration), Phys. Lett. **B461** (1999) 387; S. Ahlen et al. (AMS Collaboration), Nucl. Instrum. Meth. **A350** (1994) 351.
- [25] D.A. Petyt, A study of parameter measurement in a long-baseline neutrino oscillation experiment, Thesis submitted to Univ. of Oxford, UK, 1998.
- [26] M. Apollonio et al. (CHOOZ Collaboration), preprint hep-ex/9907037.
- [27] M.C. Gonzalez Garcia and C. Peña Garay, these proceedings, and preprint hep-ph/0001129.
- [28] G. L. Fogli, E. Lisi, A. Marrone and G. Scioscia, Phys. Rev **D59** (1999) 033001 and preprint hep-ph/9904465.
- [29] A. de Rújula, M.B. Gavela and P. Hernández, preprint hep-ph/0001124.
- [30] A. de Rújula, M.B. Gavela and P. Hernández, Nucl. Phys. **B547** (1999) 21.
- [31] A. Donini, M. B. Gavela, P. Hernández and S. Rigolin, preprint hep-ph/9909254.
- [32] J. Arafune, M. Koike and J. Sato, Phys. Rev. **D56** (1997) 3093, Erratum ibid. **D60** (1999) 119905; M. Tanimoto, Prog. Theor. Phys. **97** (1997) 9091; Phys. Lett. **B435** (1998) 373; Phys. Lett. **B462** (1999) 115; H. Minakata and H. Nunokawa, Phys. Lett. **B413** (1997) 369; Phys. Rev. **D57** (1998) 4403; S.M. Bilenky, C. Giunti and W. Grimus, preprint hep-ph/9705300; Phys. Rev. **D58** (1998) 033001; K.R. Schubert, preprint hep-ph/9902215; J. Bernabéu, preprint hep-ph/9904474; H. Fritzsch and Z.Z. Xiang, preprint hep-ph/9909304; K. Dick, M. Freund, M. Lindner and A. Romanino, Nucl. Phys. **B562** (1999) 29; A. Romanino, preprint hep-ph/9909425; M. Koike and J. Sato, preprint hep-ph/9909469; J. Sato, preprint hep-ph/9910442.
- [33] M. Campanelli, A. Bueno and A. Rubbia, Matter effects with very long baselines at the neutrino factory, these proceedings.

- [34] M. Freund, M. Lindner, S.T. Petcov and A. Romanino, preprint hep-ph/9912457; Very long baseline neutrino oscillation experiments and the MSW effect, these proceedings.
- [35] A. Cervera et al., Golden measurements at a neutrino factory, preprint CERN-TH/2000-40 (FTUAM-00-03, IFT-UAM/CSIC-00-04, FTUV/00-12, IFIC/00-13), preprint hep-ph/0002108.
- [36] I.M. Papadopoulos, Limit on the muon beam divergence at a neutrino factory, these proceedings.
- [37] C. Crisan and S. Geer, How well do we need to know the beam properties at a neutrino factory?, report FERMILAB-TM-2101.
- [38] F. Dydak, Contribution to the NuFact'99 workshop, unpublished.
- [39] N. Mokhov, Contribution to the NuFact'99 workshop, unpublished.
- [40] P. Gruber, Contribution to the NuFact'99 workshop, unpublished.
- [41] A. Blondel, Energy calibration by spin precession, in Prospective study of muon storage rings at CERN, Report CERN 99-02 (1999) and ECFA 99-197, eds. B. Autin, A. Blondel and J. Ellis, p. 51 ff.
- [42] P. Migliozi and P. Strolin, Considerations on  $\nu_\mu \leftrightarrow \nu_\tau$  appearance experiments using the emulsion technique, these proceedings.
- [43] D. A. Harris and A. Para, Neutrino oscillation appearance experiment using nuclear emulsion and magnetized iron, these proceedings.
- [44] M. Campanelli, A. Bueno and A. Rubbia,  $\nu_\mu \leftrightarrow \nu_\tau$  oscillation appearance with kinematic approach at very long baselines (VLBL), these proceedings.
- [45] J. Panman, Contribution to the NuFact'99 workshop, unpublished.
- [46] R. Edgecock, Potential of MINOS at a neutrino factory, these proceedings.
- [47] P. J. Litchfield, Atmospheric neutrinos in MINOS, these proceedings.
- [48] A. Cervera, F. Dydak and J.J. Gómez Cadenas, A large magnetic detector for the neutrino factory, these proceedings.
- [49] A. Donini, M.B. Gavela, P. Hernández and S. Rigolin, preprint hep-ph/9910516.
- [50] R. Gandhi, C. Quigg, M. Hall Reno and I. Sarcevic, *Astropart. Phys.* **5** (1996) 81.
- [51] M. de Jong, Neutrino physics at the muon collider, these proceedings.
- [52] K. McFarland, Nucleon structure, weak interactions, neutrino properties: where do we stand and where do we want to go?, these proceedings.
- [53] B. King, High rate neutrino detectors for neutrino factories, these proceedings.
- [54] P. Perez, Measurements of neutrino cross-sections with a near detector, these proceedings.
- [55] Y. Kuno, Physics opportunities of a very intense low-momentum muon source, these proceedings.